Hyperfine Interact
DOI 10.1007/s10751-013-0875-9

Magnetic and Mössbauer studies of fucan-coated magnetite nanoparticles for application on antitumoral activity

V. A. J. Silva · P. L. Andrade · Angel Bustamante · L. de los Santos Valladares · M. Mejia · I. A. Souza · K. P. S. Cavalcanti · M. P. C. Silva · J. Albino Aguiar

Abstract Fucan-coated magnetite (Fe_3O_4) nanoparticles were synthesized by the co-precipitation method and studied by Mössbauer spectroscopy and magnetic measurements. The sizes of the nanoparticles were 8–9 nm. Magnetization measurements

Proceedings of the Thirteenth Latin American Conference on the Applications of the Mössbauer Effect, (LACAME 2012), Medellín, Columbia, 11–16 November 2012.

V. A. J. Silva · P. L. Andrade · J. Albino Aguiar
Programa de Pós-Graduação em Ciências de Materiais, CCEN, Universidade Federal de Pernambuco, Av. Prof. Moraes Rego s/n, Cidade Universitária, Recife, PE, CEP 50670-901, Brazil

V. A. J. Silva (✉) · P. L. Andrade · M. P. C. Silva
Laboratório de Imunopatologia Keizo Asami (LIKA), Departamento de Bioquímica, Universidade Federal de Pernambuco, Av. Prof. Moraes Rego s/n, Cidade Universitária, Recife, PE CEP 50670-901, Brazil
e-mail: valdeene@hotmail.com

A. Bustamante · M. Mejia
Laboratorio de Cerámicos y Nanomateriales, Facultad de Ciencias Físicas, Universidad Nacional Mayor de San Marcos, Ap. Postal 14-0149, Lima, Peru

L. de los Santos Valladares · J. Albino Aguiar
Departamento de Física, Universidade Federal de Pernambuco, Av. Prof. Moraes Rego s/n, Cidade Universitária, Recife, PE CEP 50670-901, Brazil

L. de los Santos Valladares
Cavendish Laboratory, Department of Physics, University of Cambridge, J.J. Thomson Avenue, Cambridge, CB3 0HE, UK

I. A. Souza
Departamento de Antibióticos, Universidade Federal de Pernambuco, Av. Prof. Moraes Rego s/n, Cidade Universitária, Recife, PE CEP 50670-901, Brazil

K. P. S. Cavalcanti
Hospital das Clínicas, Universidade Federal de Pernambuco, Av. Prof. Moraes Rego s/n, Cidade Universitária, Recife, PE CEP 50670-901, Brazil

Published online: 23 July 2013

and Mössbauer spectroscopy at 300 K revealed superparamagnetic behavior. The magnetic moment of the Fe_3O_4 is partly screened by the Fucan coating aggregation. When the magnetite nanoparticles are capped with oleic acid or fucan, reduced particle-particle interaction is observed by Mössbauer and TEM studies. The antitumoral activity of the fucan-coated nanoparticles were tested in Sarcoma 180, showing an effective reduction of the tumor size.

Keywords Magnetic nanoparticles · Magnetite · Fucan · Antitumoral activity

1 Introduction

Currently, magnetic nanoparticles (MNPs) are widely used in the fields of biology and medicine, such as protein and enzyme immobilization, bioseparation, immunoassay, hyperthermia, drug delivery, magnetically enhanced transfection, tissue engineering and magnetic resonance imaging (MRI) [1–5]. Magnetic nanoparticles are usually composed of magnetic elements, such as iron, nickel, cobalt and their respective oxides [6–8]. Iron oxides, such as magnetite (Fe_3O_4), are biodegradable, biocompatible, present stable magnetic response and superparamagnetic effects [9, 10]. Magnetite has recently attracted attention because it has a high Curie temperature (T_C ~850 K) and nearly full spin polarization at room temperature. Both properties are of great potential for applications in giant magnetoelectronic and spin-valve devices based on magnetite films [11]. Mössbauer and magnetic studies performed in magnetite confirms that the iron cations in Fe_3O_4 present two valence states, $Fe^{2.5+}$ and Fe^{3+} distributed in an inverse spinel structure (space group Fd_3m). Fe^{+3} cations locate on the tetrahedral co-ordination (FeO_4) site (A); and both Fe^{+3} and $Fe^{+2.5}$ locate on the octahedral co-ordination (FeO_6) site (B) in antiparallel arrangement, yielding ferrimagnetic order below T_C [2, 11].

Magnetite nanoparticles have reduced magnetic dipole-dipole interaction; hence, no magnetization is retained in these particles after removal of the external field. They are thus considered as superparamagnetic, and their magnetic properties are affected by coating them with different capping agents [12]. Several coating materials have been used to modify the surface chemistry of the magnetite nanoparticles, including organic polymers, organic surfactants, metals [13], oxides and bioactive molecules and structures [14]. One of the main problems in producing stable magnetic fluid consisting on individual coated magnetite nanoparticles is to prevent their agglomeration during the synthesis process [15]. In this sense, oleic acid is commonly used as surfactant to modify the surface of the magnetite particles since it has higher affinity to the surface compared to other surfactants [16].

Fucoidans are water soluble sulfated polysaccharides with high molecular weight. They are the main constituents of brown algae and can be found also in some marine invertebrates [17–20]. These complex polysaccharides show a wide variety of biological activities, such as anti-adhesive [21], anti-coagulant [22, 23], anti-complimentary [24], anti-oxidant [25], anti-proliferative [26], anti-thrombotic [27], anti-platelet aggregation [28], anti-tumor [29] and anti-viral properties [30, 31]. Thus, obtaining magnetite nanoparticles coated with polysaccharides is attractive for medical applications.

In the present work we study the influence of the Fucan coating on the magnetic properties of the magnetite nanoparticles by Mössbauer spectroscopy and magnetic measurements. The results are compared to similar works reported by other authors for magnetite coated with silica [32], oleic acid and polyethylene glycol [12, 33]. In addition, preliminary study of the antitumoral activity of coated magnetite nanoparticles is reported.

2 Methodology

2.1 Preparation of the fucan-magnetite nanoparticles

Algae *Sargassum cymosum* were dried, pulverized and immersed in 300 mL of acetone and stirred during 12 h to remove pigments and lipids. This process was repeated twice. Then, it was decanted and the residue was dried at 45 °C under aeration to obtain a Ketonic powder. Next, a solution of 0.15 M NaCl (250 mL) was added to the ketonic powder and the pH was adjusted to 8.0 with NaOH. The proteolysis of this ketonic powder was carried out by papain enzyme (15 mg/g of ketonic powder) and the mixture was incubated at 45 °C overnight. The supernatant was collected by centrifugation at 10,000 × g for 10 min and dried in a lyophilizer Multi-Tainer (FTS Systems, INC).

In parallel to the fucan extraction, an aqueous suspension of magnetite nanoparticles was prepared by co-precipitation of Fe(III) and Fe(II) in the presence of NH_4OH and oleic acid following standard procedure [34]. 10 mL of ferrous chloride, 10 mL of ferric chloride and 500 μL of oleic acid were added to 100 mL of distilled water under stirring. Then a NH_4OH solution was dropped to the mixture to raise the pH to 11.0 while maintaining a vigorous stirring. After this step, the mixture was heated at 85 ± 3 °C for 30 min while stirring it (7,000 rpm). The co-precipitated magnetite nanoparticles were then thoroughly washed with distilled water. The material was dried and kept at room temperature (25 °C). The coating of magnetite nanoparticles with the polysaccharide fucan was achieved by the adsorption method. The fucan solution in distilled water (50 mg/mL) was added to the obtained magnetite nanoparticles (100 mg) and maintained at 25 °C for 16 h under stirring. Afterward, the coated nanoparticles were thoroughly washed with distilled water. The material was dried and kept at room temperature (25 °C).

2.2 Characterization of the fucan-magnetite nanoparticles

The sizes of the MNPs were observed through a transmission electron microscopy (TEM, TECNAI G2 Spirit—FEI Company) with an acceleration voltage of 80 kV. For TEM analysis, the samples were deposited on copper grids of 400 mesh coated with carbon. The crystalline properties and phase identification were characterized by X-rays diffraction (XRD), using a Siemens D5000 diffractometer. The diffractogram was obtained by using Cu-Kα radiation ($\lambda = 1.5406$ Å) in the range $10° < 2\theta° < 80°$ with a step of 0.02° and acquisition time of 1.0 s/step.

The Mössbauer characterization was performed with a conventional transmission Mössbauer spectrometer, operating with 1,024 channels (after folding is 512 channels) and a Wissel INC. velocity module with a sinusoidal signal. The measurements

were taken at room temperature (RT) and the obtained data were adjusted with the help of the program NORMOS, generating the data file with the extension PLT and determining the difference between the experimental data and the calculated data. In this program, the good fitting is controlled by the value of the χ^2. The source employed was a ^{57}Co in rhodium matrix with a of 25 mCi. The isomer shift and the velocity scale were calibrated with respect to a α-Fe film at RT. The sample holder used has a diameter of 1 cm (0.7854 cm^2) which permitted to ascertain and quantify the small systematic effects of cosine smearing which usually occur in the folded Mössbauer spectra when relatively large collection solid angles are used. These conditions were appropriate to obtain a rating of 8,500 counts per second.

The magnetic properties of the magnetite nanoparticles (MNPs) were measured on a MPMS-5S (Magnetic Property Measurement System) magnetometer from Quantum Design, with sensor SQUID (Superconducting Quantum Interference Device). About 5 mg of each sample were encapsulated and mounted in the equipment rod. The measurements were taken at room temperature (25 °C) and under different applied magnetic fields from −7 to +7 kOe, and the magnetization (in emu/g) was obtained by dividing the raw magnetization by the sample mass.

2.3 Antitumoral activity in vivo

Sarcoma 180 tumor cells were subcutaneously inoculated (3×10^6 cells/mouse) into 3 months old male Swiss mice. Subsequently, the fucan-coated and uncoated magnetite nanoparticles were dissolved in saline and injected intraperitoneally (ip) once a day for 7 days, starting at 48 h after tumor inoculation. The same volume of saline was injected into the control mice. Despite the fact that magnetite was reported to have high biocompatibility without toxicity [35] the uncoated magnetite nanoparticles were injected to a mouse to confirm it and to observe possible side effects. The mice were sacrificed on the next day after the last injection, and the tumors were excised. The tumor weights were compared with those in the control mice.

3 Results and discussion

In Fig. 1a, the uncoated MNPs showed the aggregate of particles occurred since the specific surface area (surface-to-volume ratio) is large resulting in a high surface energy. After fucan coating, the aggregation was reduced and the nanoparticle dispersion was improved (see Fig. 1b). The lack of aggregation is probably caused by the fucan coatings which weaknesses the magnetic interactions between particles.

From many TEM images, 261 and 728 uncoated and coated particles respectively, with nearly spherical shape, were counted to estimate the mean diameter using the ImagJ software. Subsequently a size histogram was mounted using the Sturges method. The bin-width (W) is obtained from the relation: $W = (D_{\max} - D_{\min})/k$, where $k = 1 + 3.322 \log(\mathrm{N})$. The particle size distribution was then modeled with a log-normal distribution: $f(D) = \left(A/\sqrt{2\pi\sigma\ \ D}\right) \exp\left[-\ln^2(D/D_0)/2\sigma^2\right]$. Here the D_0 is the statistical mean diameter, A is a constant to be determined by fitting the statistical distribution and σ represents the degree of polydisperion. The mean value and its standar deviation are given by $\langle D\rangle = D_0 e^{\sigma^2}/2$ and $\sigma_D = \langle D\rangle \sqrt{e^{\sigma^2} - 1}$, respectively. The histogram distribution of the size for the uncoated and coated

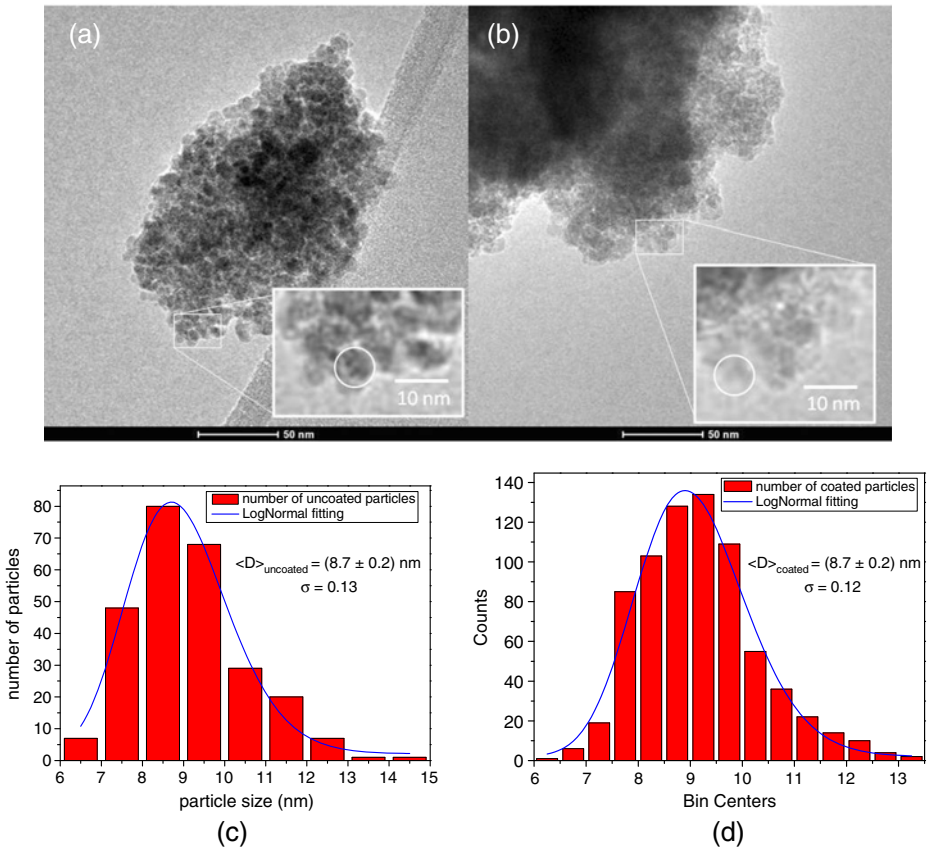

Fig. 1 **a** TEM micrograph of the uncoated MNPs, **b** TEM micrograph of fucan- coated MNPs and histogram of the size distributions of the uncoated **c** and Fucan-coated **d** Nanoparticles

nanoparticles are shown in Fig. 1c and d respectively. Table 1 list the statistical values obtained during fitting. Note that in the table, the coated nanoparticles are slightly bigger than the uncoated ones due to the presence of the Fucan.

Figure 2 shows the XRD of the uncoated magnetite nanoparticles, magnetite-oleic acid nanoparticles, magnetite-fucan nanoparticles and magnetite-oleic acid-fucan nanoparticles. The principal reflections (220), (311), (400), (422), (511) and (440) were indexed with the PDF card No 85-1436. From the line broadening of the diffraction peaks the particle size were determined using the Scherrer formula $D = \frac{0.916\lambda}{\beta_{\mathrm{hkl}} \cos\theta_{\mathrm{hkl}}}$ where $\lambda = 1.5406$ Å is the wavelength of the applied X-ray radiation ($K_{\alpha 1}$ radiation of copper), β_{hkl} is the pure diffraction line broadening (in radians), which can be easily found by measuring the full width at half maximum (FWHM) of the principal hkl reflections and θ_{hkl} is the Bragg angle. In order to obtain more accurate estimations on the Scherrer formula, each peak was fitted with Gaussian functions and levelling the background in each diffractogram to zero. For example, Fig. 2b and c show the (311) reflections of the uncoated and Fucan-coated samples. Note that the diffractogram for the coated sample is more dispersed due to the

Table 1 Statistical values obtained after fitting the histogram distribution of the N = 261 and 728 uncoated and coated nanoparticles respectively taken from the TEM micrographs

	N	$<D>$ (nm)	D_0	Σ	A
Uncoated	261	8.7 ± 0.2	8.8	0.13	242.21
Coated	728	8.9 ± 0.2	9.0	0.11	348.98

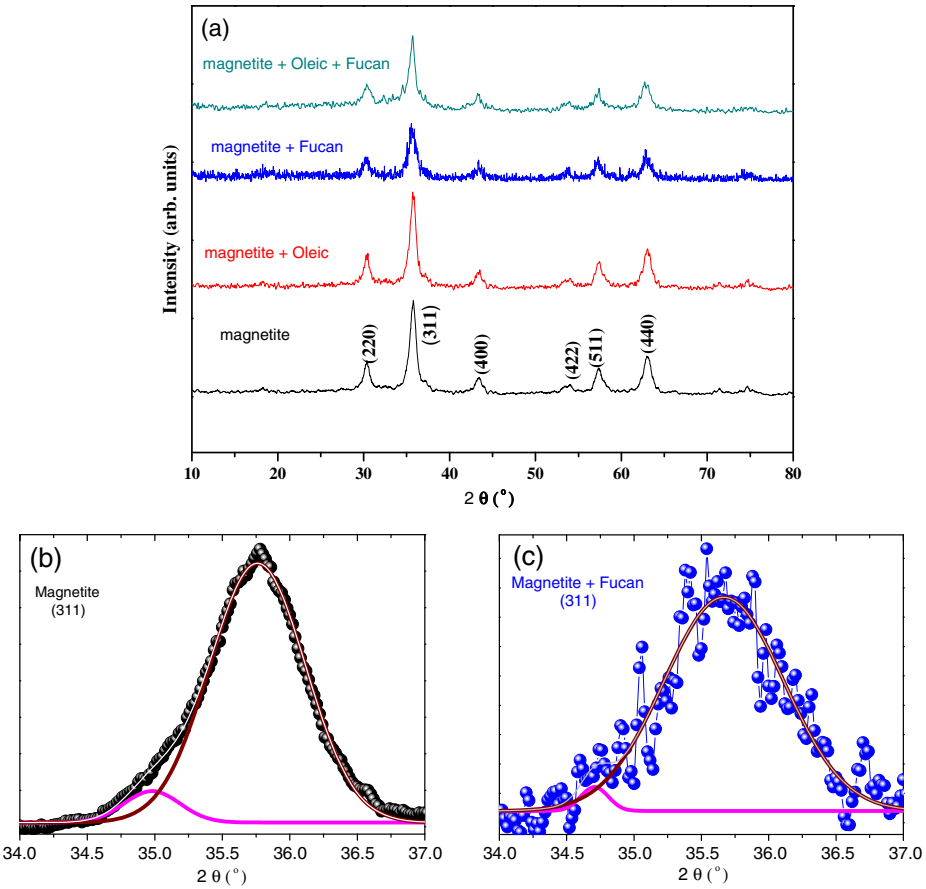

Fig. 2 **a** X-ray diffraction patterns of the Fe_3O_4 samples with different shells, **b** (311) peak for magnetite **c** (311) peak for magnetite-fucan

presence of the organic shells. Table 2 show the calculated average sizes for the four samples. The average sizes for the uncoated and Fucan-coated particles are 8.5 and 8.7 nm respectively, which are very close to those values estimated in the TEM images above.

The measurements of the magnetization with the applied magnetic field, M(H), of the uncoated and fucan-coated magnetite nanoparticles at 300 K are presented in Fig. 3. The magnetization values were obtained by dividing the raw data provided by the DC-MPMS magnetometer by the sample mass, thus in the case of the fucan-coated nanoparticles, these values correspond to the raw data divided by the total

Table 2 Average size of the crystallites obtained from the principal peaks on the XRD of the uncoated and coated magnetite particles

Hkl	Magnetite grain size (nm)	Magnetite + oleic acid grain size (nm)	Mag + fucan grain size (nm)	Mg + F+ oleic acid grain size (nm)
220	8.4	8.9	8.6	9.1
311	8.7	9.9	9.0	13.4
400	8.3	8.0	8.6	9.6
511	8.4	7.8	8.6	10.5
440	8.5	10.2	8.5	9.3
Mean size (nm)	8.5	8.9	8.7	10.4

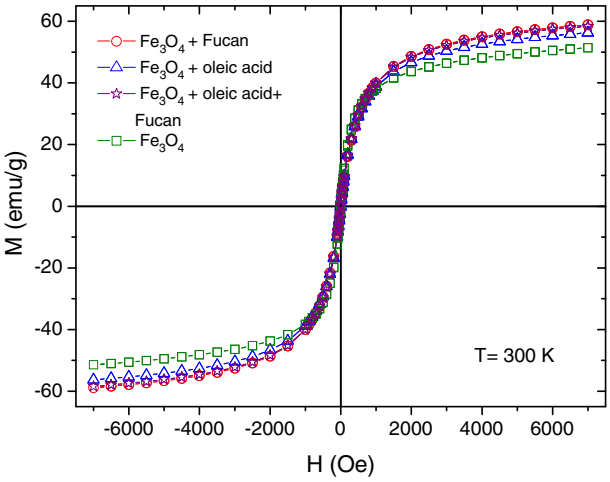

Fig. 3 Magnetization (M) curves as the function of the applied magnetic field (H) of the Fe_3O_4 nanoparticles

mass (about 5 mg). In this way, the mass of the core magnetite in each sample are slightly different. Since we can not estimate the mass of the organic material, the data provided for the coated particles in the figure should be considered only as a first approximation.

The plots are typical from superparamagnetic iron nanoparticles with almost zero remanence and coercivity [11]. The superparamagnetic behavior is mainly generated by the magnetite cores in each sample. At 300 K, the saturation magnetization (M_S), determined by using the law of approach to saturation (a linear term is included in order to account for the linear increase of M at high fields), is around 52 emu/g for the uncoated Fe_3O_4 NPs. This saturation magnetization value is consistent with the value reported in the literature for uncoated magnetite NPs with sizes smaller than 10 nm [11]. The saturation value for the uncoated sample should be considered as a first approximation (see above).

Figure 4a shows the Mössbauer spectra at RT of the uncoated magnetite nanoparticles and its correspondent hyperfine magnetic field distribution. The spectrum of the magnetite nanoparticles show one sextet with broadened line width and it was fitted with one hyperfine magnetic field distributions with $\chi^2 \sim 1.47$, showing a principal most probably magnetic field of 46.10 T due to magnetic relaxation of magnetite nanoparticles. In this case, the magnetic moment of an individual particle fluctuates through the most easy axis of magnetization during a time $\tau = \tau_0 \exp(KV/k_BT)$,

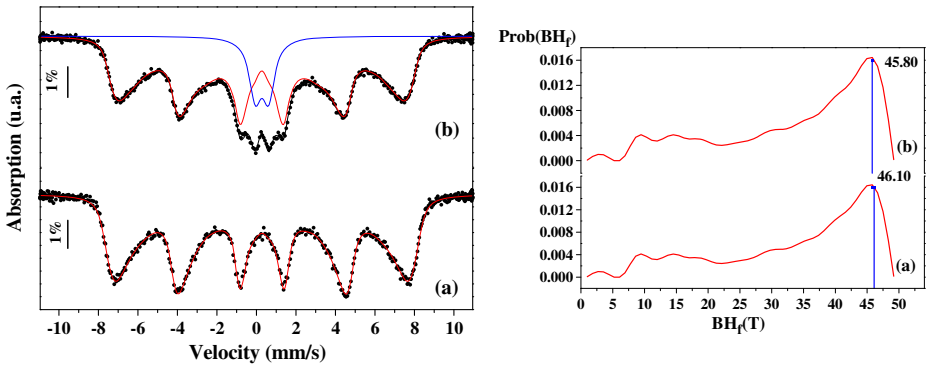

Fig. 4 Mossbauer spectra at RT. **a** Uncoated nano-magnetite particles and **b** Fucan coated nano-magnetite. The hyperfine magnetic field distributions are on the *right* panel

where K is the magnetic anisotropy constant, V is the volume of the particle, k_B is the Boltzmann constant, T is the temperature and τ_0 is a constant characteristic of the material. Therefore, for a fluctuation time longer than the characteristic Mössbauer time (10^{-8} s), magnetically splitted spectra can be measured due slow relaxation. The hyperfine parameters are shown in the Table 3.

Figure 4b show the Mössbauer spectra at RT of the magnetite nanoparticles coated with fucan polysacharides and its corresponding hyperfine magnetic field distribution. The spectrum was fitted in first approximation using one distribution and one doublet with $\chi^2 \sim 1.38$, showing an asymmetrically broadened spectra. This is originated by a complex mixture of static and dynamic broadenings due to the broad size distribution and the strength of interparticle interactions with slow particles (sextet with area of 87.1 %) and rapid particles (the doublet SP with area of 12.9 %). In this way, a reduced magnetic dipole-dipole interaction is produced by the coated fucan as observed in magnetization measurements (Fig. 3) and also in other systems [34]. The hyperfine magnetic field distribution shows a principal magnetic field most probably of 45.80 T.

Figure 5 shows the Mössbauer spectra at RT of the oleic acid-magnetite nanoparticles and fucan-oleic acid- magnetite nanoparticles. In the case of the Mössbauer spectra of the magnetite coated with oleic acid + fucan polysacharides, the coating minimizes the interactions between particles which are reflected in a diminution of the hyperfine field, showing a superposition of one hyperfine field distribution and one doublet, with a principal magnetic field most probably of 13.3 T and area of 71.3 % due to magnetic relaxation of magnetite nanoparticles. The doublet would be magnetic collective excitations or superparamagnetic signal with $QS = 0.68$ mm/s, $\delta = 0.389$ mm/s and 28.7 %.

While the Mössbauer spectra of the magnetite coated with oleic acid, the spectrum is typical of magnetic nanoparticles with weak dipole-dipole interaction. The presence of a doublet of 17.7 % area in contrast to the hyperfine field distribution $P(B_{hf})$ of 82.3 % area indicates the superparamagnetic effect has intensified. The Mössbauer spectrum of the magnetite nanoparticles coated with fucan and oleic acid is similar to the previous one. However in this case it seems that the magnetic distribution of the

Table 3 Mössbauer hyperfine parameters obtained at RT

Samples - sites	δ (mm/s)	ε, Δ (mm/s)[a]	B_{hf} (Tesla)	Area (%)
Magnetite Dist. Fe^{3+}-$Fe^{2.5+}$	0.391	−0.01	46.10	100.0
Magnetite with fucan Dist				
Fe^{3+}-$Fe^{2.5+}$	0.380	0.00	45.80	87.1
Doublet SP	0.390	0.67	–	12.9
Magnetite with oleic acid				
Dist	0.403	−0.01	44.8	82.3
Doublet SP	0.395	0.63	–	17.7
Magnetite with oleic acid				
and fucan Dist	0.386	−0.02	13.3	71.3
Doublet SP	0.389	0.68	–	28.7

[a]Representing the superparamagnetic doublet
δ is the isomer shift relative to α-iron, ε and Δ is the quadrupole splitting and *A* is the spectral fraction as obtained from the fit. B_{hf} is the hyperfine field. *SP* Superparamagnetic

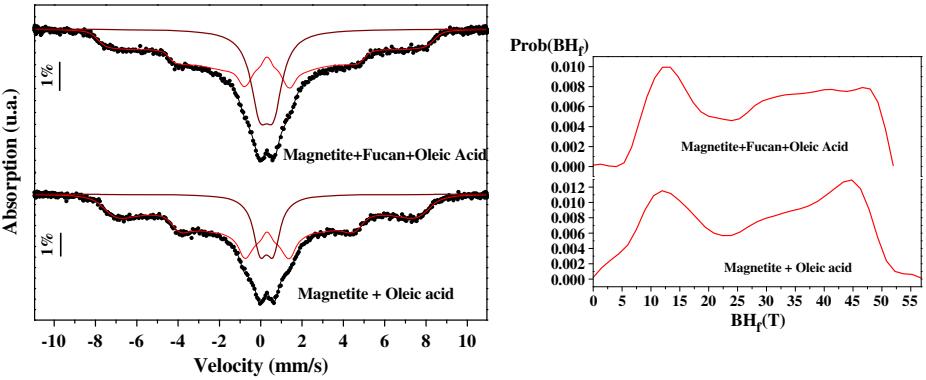

Fig. 5 Mössbauer spectra at RT for oleic acid-magnetite nanoparticles and fucan-oleic acid- magnetite nanoparticles. *Solid lines* are the best fits using hyperfine field distributions $P(B_{hf})$ shown on the *right panel*

surface affects the anisotropy energy and the doublet increases in area (to 28.7 %) whereas the hyperfine field distribution $P(B_{hf})$ area is 71.3 %

The magnetite-fucan nanoparticles were applied in vivo to analyse the antitumoral activity of Sarcoma 180. The samples of pure fucan and a control group with only saline solution were also applied. In Fig. 6, we can observed the Sarcoma 180 tumor after treated by saline as control (A), by magnetite nanoparticles (B) and by fucan-magnetite nanoparticles (C). It is observed that the magnetite nanoparticles not presented antitumoral effect (Fig. 6b), but in Fig. 6c he tumor size is reduced, demonstrating that fucan-magnetite nanoparticles are effective in the antitumoral treatment for Sarcoma 180. The animals that were treated with pure fucan injection, died within the 24 h after the application. Our research group is currently performing more tests in vivo and in vitro in order to understand better what happened. However, up to date is is assumed that the pure fucan killed the animals due a hyperestimulation immunology.

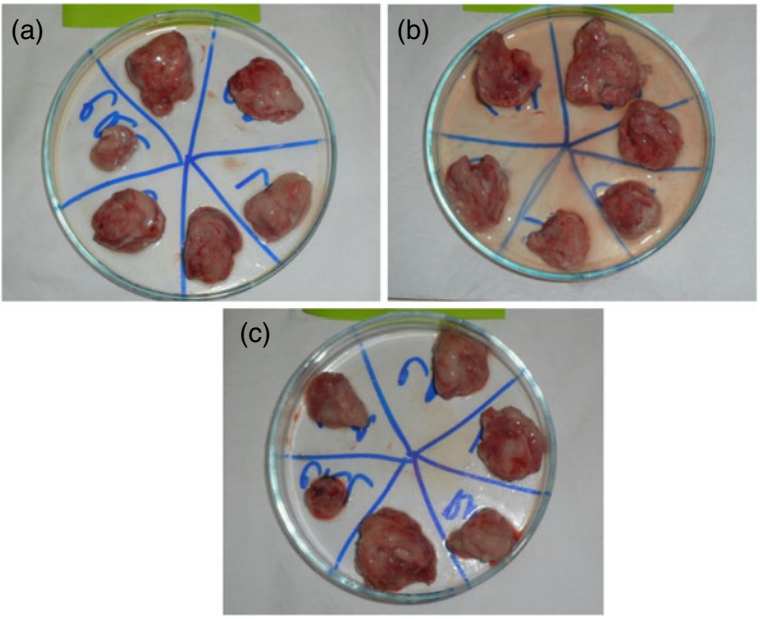

Fig. 6 In vivo effect of **a** Control, **b** Magnetite nanoparticles and **c** Fucan-magnetite nanoparticles in Sarcoma 180

4 Conclusions

In summary, the magnetic measurements and Mössbauer spectroscopy at RT revealed that the superparamagnetic property of the Fe_3O_4 nanoparticles is affected by the fucan polysaccharide and oleic acid coating, thus preventing aggregation. The fucan-magnetite nanoparticles are promising for the treatment of the Sarcoma 180 tumor size.

Acknowledgements This work was supported by the Brazilian science agencies Coordenação de Aperfeiçoamento de Pessoal de Nível Superior (CAPES), Conselho Nacional de Desenvolvimento Científico e Tecnológico (CNPq) and the Fundação de Amparo à Ciência e Tecnologia do Estado de Pernambuco (FACEPE) (APQ-0589-1.05/08).

References

1. Zhang, L.Y., Zhu, X.J., Sun, H.W., Chi, G.R., Xu, J.X., Sun, Y.L.: Control synthesis of magnetic Fe_3O_4–chitosan nanoparticles under UV irradiation in aqueous system. Curr. Appl. Phys. **10**, 828–833 (2010)
2. Zhan, Y., Meng, F., Yang, X., Zhao, R., Liu, X.: Solvothermal synthesis and characterization of functionalized graphene sheets (FGSs)/magnetite hybrids. Mater. Sci. Eng. B. **176**, 333–1339 (2011)
3. Corchero, J., Villaverde, A.: Biomedical applications of distally controlled magnetic nanoparticles. Trends Biotechnol. **27**, 468–76 (2009)
4. Rahimi, M., Wadajkar, A., Subramanian, K., Yousef, M., Cui, W., Hsieh, J., Nguyen, K.: In vitro evaluation of novel polymer-coated magnetic nanoparticles Q13 for controlled drug delivery. Nanomedicine **6**, 672–680 (2010)

5. de los Santos Valladares, L., Llandro, J., Lee, D., Mitrelias, T., Palfreyman, J.J., Hayward, T.J., Cooper, J., Bland, J.A.C., Barnes, C.H.W., Arroyo, J.L., Lees, M.: Magnetic measurements of suspended functionalised ferromagnetic beads under DC applied fields. J. Magn. Magn. Mater. **321**, 2129–2134 (2009)
6. Shubayev, V.I., Pisanic, T.R., Jin, S.: Magnetic nanoparticles for theragnostics. Adv. Drug Deliv. Rev. **61**, 467–477 (2009)
7. Andrade, P.L., Silva, V.A.J., Maciel, J.C., Santillan, M.M., Moreno, N.O., De Los Santos Valladares, L., Bustamante Domínguez, A., Pereira, S.M.B., Silva, M.P.C., Albino Aguiar, J.: Preparation and characterization of cobalt ferrite nanoparticles coated with fucan and oleic acid. Hyperfine Interact. doi:10.1007/s10751-013-0835-4
8. Ramos, J.A., Bustamante Domínguez, A., Flores Santibañez, J., Mejia, M., Osorio Anaya, A., Martínez, A.I., De Los Santos Valladares, L., Barnes, C.H.W.: Mössbauer study of intermédiate superparamagnetic relaxation of maghemite (γ-Fe2O3) nanoparticles. Hyperfine Interact. doi:10.1007/s10751-013-0864-z
9. Jain, T.K., Richey, J., Strand, M., Leslie-Pelecky, D.L., Flask, C.A., Labhasetwar, V.: Magnetic nanoparticles with dual functional properties: drug delivery and magnetic resonance imaging. Biomaterials **29**, 4012–4021 (2008)
10. Kumar, A., Prasanna, K.J., Behera, S., Lockey, R.F., Monapatra, S.M., Shy, A.M.: Multifunctional magnetic nanoparticles for targeted delivery. Nanomedicine **6**, 64–69 (2010)
11. Goya, G.F., Berquó, T.S., Fonseca, F.C., Morales, M.P.: Static and dynamic magnetic properties of spherical magnetite nanoparticles. J. Appl. Phys. **94**, 3520–3528 (2003)
12. Mikhaylova, M., Kim, D.K., Bobrysheva, N., Osmolowsky, M., Semenov, V., Tsakalakos, T., Muhammed, M.: Superparamagnetism of magnetite nanoparticles: dependence on surface modification. Langmuir **20**, 2472–2477 (2004)
13. León Félix, L., Chaker, J., Parise, M., Coaquira, J.A.H., de los Santos Valladares, L., Bustamante, A., Garg, V.K., Oliveira, A.C., Morais, P.C.: Synthesis and characterization of uncoated and gold-coated magnetite nanoparticles. Hyperfirne Interact. doi:10.1007/s10751-013-0857-y
14. Cabrera, L., Gutierrez, S., Menendez, N., Morales, M.P., Herrasti, P.: Magnetite nanoparticles: electrochemical synthesis and characterization. Electrochim. Acta **53**, 3436–3441 (2008)
15. Kim, D.K., Zhang, Y., Voit, W., Rao, K.V., Muhammed, M.: Synthesis and characterization of surfactant-coated superparamagnetic monodispersed iron oxide nanoparticles. J. Magn. Magn. Mater. **225**, 30–36 (2001)
16. Yang, K., Peng, H., Wen, Y., Li, N.: Re-examination of characteristic FTIR spectrum of secondary layer in bilayer oleic acid-coated Fe3O4 nanoparticles. Appl. Surf. Sci. **256**, 3093–3097 (2010)
17. Araujo, P.M., Oliveira, G.B., Cordula, C.R., Leite, E.L., Carvalho, L.B., Silva, M.P.C.: Sulfated fucan as support for antibiotic immobilization. Braz. J. Med. Biol. Res. **37**, 301–305 (2004)
18. Yoon, S.J., Pyun, Y.R., Wang, J.K.H., Moura, P.A.S.: A sulfated fucan from the brown alga Laminaria cichorioides has mainly heparin cofactor II dependent anticoagulant activity. Carbohydr. Res. **342**, 2326–2330 (2007)
19. Queiroz, K.C.S., Medeiros, V.P., Queiroz, L.S., Abreu, L.R.D., Rocha, H.A.O., Ferreira, C.V., Juca, M.B., Aoyama, H., Leite, E.L.: Inhibition of reverse transcriptase activity of HIV by polysaccharides of brown algae. Biomed. Pharmacother. **62**, 303–30 (2008)
20. Karmakar, P., Ghosh, T., Sinha, S., Saha, S., Mandal, P., Ghosal, P.K., Ray, B.: Polysaccharides from the brown seaweed Padina tetrastromatica: characterization of a sulfated fucan. Carbohyd. Polym. **78**, 416–421 (2009)
21. McCormick, C.J., Newbold, C.I., Berendt, A.R.: Sulfated glycoconjugatesenhance CD36-dependent adhesion of Plasmodium falciparum-infectederythrocytes to human microvascular endothelial cell. Blood **96**, 327–333 (2000)
22. Cumashi, A., Ushakova, N.A., Preobrazhenskaya, M.E., D'Incecco, A., Piccoli, A., Totani, L.: A comparative study of the anti-inflammatory, anticoagulant, anti-angiogenic and anti-adhesive activities of nine different fucoidans from brown seaweeds. Glycobiology **17**, 541–552 (2007)
23. Mourão, P.A.S.: Use of sulfated fucans as anticoagulant and antithrombicagents: future perspective. Curr. Pharm. Des. **10**, 967–981 (2004)
24. Tissot, B., Daniel, R.: Biological properties of sulfated fucans: the potent inhibiting activity of algal fucoidan against the human complement system. Glycobiology **13**, 29G–31G (2003)
25. Chew, Y.L., Lim, Y.Y., Omar, M., Khoo, K.S.: Antioxidant activity of three edible seaweeds from two areas in South East Asia. LWT-Food Sci. Technol. **41**, 1067–1072 (2008)

26. Patel, M.K., Mulloy, B., Gallagher, K.L., O'Brien, L., Hughes, A.D.: The antimitogenic action of the sulfated polysaccharide sulfated fucan differs from heparin in human vascular smooth muscle cells. Thromb. Haemost. **87**, 149–154 (2002)
27. Nishino, T., Fukuda, A., Nagumo, T., Fujihara, M., Kaji, E.: Inhibition of the generation of thrombin and factor Xa by a sulfated fucan from the brown seaweed Ecklonia kurome. Thromb. Res. **96**, 37–49 (1999)
28. Alwayn, I.P., Appel, J.Z., Goepfert, C., Buhler, L., Cooper, D.K., Robson, S.C.: Inhibition of platelet aggregation in baboons: therapeutic implications for xenotransplantation. Xenotransplantation **7**, 247–257 (2000)
29. Alekseyenko, T.V., Zhanayeva, S.Y., Venediktova, A.A., Zvyagintseva, T.N., Kuznetsova, T.A., Besednova, N.N.: Antitumor and antimetastatic activity of fucoidan, a sulfated polysaccharide isolated from the Okhotsk sea Fucus evanescens brown alga. Bull. Exp. Biol. Med. **147**, 730–732 (2007)
30. Ghosh, T., Chattopadhyay, K., Marschall, M., Karmakar, P., Mandal, P., Ray, B.: Focus on antivirally active sulfated polysaccharides: from structure activity analysis to clinical evaluation. Glycobiology **19**, 2–15 (2009)
31. Chandia, N.P., Matsuhiro, B.: Characterization of a fucoidan from Lessonia vadosa (Phaeophyta) and its anticoagulant and elicitor properties. Int. J. Biol. Macromol. **42**, 235–240 (2008)
32. Ferreira, R.V., Pereira, I.L.S., Cavalcante, L.C.D., Gamarra, L.F., Carneiro, S.M., Amaro Jr., E., Fabris, J.D., Domingues, R.Z., Andrade, A.L.: Synthesis and characterization of silica-coated nanoparticles of magnetite. Hypefine Interact. **195**, 265–274 (2010)
33. Ghosh, R., Pradhan, L., Devi, Y.P., Meena, S.S., Tewari, R., Amit, A.K., Sharma, S., Gajbhiye, N.S., Vatsa, R.K., Pandey, B.N., Ningthoujam, R.S.: Induction heating studies of Fe_3O_4 magnetic nanoparticles capped with oleic acid and polyethylene glycol for hyperthermia. J. Mater. Chem. **21**, 13388 (2011)
34. Carneiro Leão, A.M.A., Oliveira, E.A., Carvalho Jr., L.B.: Immobilization of protein on ferromagnetic dacron. Appl. Biochem. Biotechnol. **32**, 53–58 (1991)
35. Theerdhala, S., Bahadur, D., Vita, S., Perkas, N., Zhong, Z., Gedanken, A.: Sonochemical stabilization of ultrafine colloidal biocompatible magnetite nanoparticles using amino acid, L-arginine, for possible bio applications. Ultrason. Sonochem. **17**, 730–737 (2010)